This study investigates dynamic interaction between the soil and an obstacle under explosive loading. The task addressed is to protect underground structures with shallow laying in the soil massif from the effect of critical explosive influences, which is becoming increasingly relevant under conditions of military threats.

A methodology has been devised to numerically solve the problem of a cylindrical warhead explosion on the surface of the soil massif, taking into account the interaction with the foundation-cement obstacle. That has made it possible to investigate the patterns of change in wave processes in the soil and obstacle depending on time, charge mass, and depth of the screen.

The wave interaction between the explosion and the soil massif with an obstacle was numerically simulated. The isobar field was determined at different times and velocity isoseisms were defined, which show the dynamics of wave propagation deep into the soil massif and changes in their velocity. Dependences of the peak stress on the depth for different warhead masses (50, 150, and 500 kg) were derived, as well as the resulting peak stresses and the minimum safe horizontal distances to the epicenter of the explosion for the obstacle. The dependences between the deflection and pressure of the protective soil-cement structure were determined, which makes it possible to predict the stability of the protective screen at its different thickness.

It has been established that the peak stress decreases rapidly with distance from the epicenter of the explosion. For $R < 3.7$ m, the screen (obstacle) is in the zone of high tensile stresses ($\sigma_{max} > 2$ MPa), which leads to crushing, loss of shape, and stability of the structure. For $R \approx 7.4$ m, the tensile stress decreases to approximately 0.3–0.5 MPa. These values should be considered as a threshold value for maintaining the holding (protective) function of the soil-cement obstacle.

A nomogram has been constructed to assess the mechanical properties of a soil-cement barrier located at a certain depth during a surface explosion of a warhead of different mass depending on the cement content. This facilitates practical management of the stability of the protective structure by adjusting the parameters of the bonding mixture.

The prospects of engineering protection of underground facilities by forming a continuous soil-cement screen in the path of the blast wave, formed by jet cementing of soils, have been proven

Keywords: blast waves, soil massif, soil-cement screen, mathematical modeling, stability prediction

UDC 622+502/504
DOI: 10.15587/1729-4061.2026.358194

ASSESSING THE STABILITY OF A PROTECTIVE SOIL-CEMENT STRUCTURE IN THE SOIL MASSIF UNDER THE ACTION OF CRITICAL EXPLOSIVE IMPACTS

Natalia Remez
Doctor of Technical Sciences*
ORCID: https://orcid.org/0000-0002-8646-6527
Hennadii Haiko
Doctor of Technical Sciences*
ORCID: https://orcid.org/0000-0002-4263-5958
Vadym Bronytskyi
Corresponding author
PhD*
E-mail: Vadym.Bronytskyi@lll.kpi.ua
ORCID :https://orcid.org/0000-0002-3092-3418
Tetiana Hrebeniuk
PhD*
ORCID: https://orcid.org/0000-0002-9287-2919
Svitlana Haiko
Doctor of Philosophy (PhD)
Institute of Telecommunications and Global Information Space of the National Academy of Sciences of Ukraine
Chokolivskyi bulv., 13, Kyiv,Ukraine, 03186
ORCID: https://orcid.org/0000-0002-3564-475X
*Department of Geoengineering
National Technical University of Ukraine "Igor Sikorsky Kyiv Polytechnic Institute"
Beresteiskyi ave., 37, Kyiv, Ukraine, 03056

Received 03.02.2026
Received in revised form 02.03.2026
Accepted 17.04.2026
Published 30.04.2026

How to Cite: *Remez, N., Haiko, H., Bronytskyi, V., Hrebeniuk, T., Haiko, S. (2026). Assessing the stability of a protective soil-cement structure in the soil massif under the action of critical explosive impacts. Eastern-European Journal of Enterprise Technologies, 2 (7 (140)), 62–71. https://doi.org/10.15587/1729-4061.2026.358194*

1. Introduction

Protecting civilians and critical infrastructure under conditions of military threats requires extensive development of urban underground space in order to construct new protective facilities (in particular, civil defense facilities). In addition, it is also possible to use existing underground facilities, which, if necessary, could serve to protect people from air strikes, providing the functions of dual-purpose facilities [1–3].

The task of ensuring the stability of underground facilities under the influence of external explosions is critically important for civil, military, and industrial infrastructure at different stages of their life cycle – from design and construction to operation. This issue is especially acute under conditions of full-scale military hostilities. To ensure the reliability of shallow-laid civil defense facilities from critical explosive effects (direct hit of warheads into the perimeter of an underground facility), special engineering protection is required. Among the promising ways of such protection are the solid soil-cement structures (screens), formed by jet cementing of soils to the required depth and placed in the path of the blast wave [3–5].

Unlike above-ground structures, underground facilities respond to explosive loading indirectly – through a dynamic

seismic wave propagating through the soil [6]. An external explosion near the earth's surface generates an air shock wave, which is transformed into a stress wave in the soil mass. The intensity and nature of this wave depend on the mass of the charge, distance, depth of the structure, physical and mechanical properties of the soil, as well as the presence of obstacles [7]. Assessment of critical explosive effects on the soil mass and soil-cement obstacle opens up new opportunities for controlling the parameters of engineering protection of underground objects of critical infrastructure and civil defense under conditions of active military operations.

The above renders relevance to studies aimed at predicting the stability of a protective soil-cement structure in a soil massif under the action of critical explosive influences.

2. Literature review and problem statement

Paper [8] reports a study on the peak pressure P_{max} and impulse I of an explosion wave in the soil depending on the scaled distance Z by using classical methods that employ empirical and semi-empirical dependences. However, this approach does not make it possible to obtain regularities in the evolution of wave processes for different soil conditions and explosion parameters.

An option for overcoming corresponding difficulties is to use mass, momentum, and energy conservation equations. This is the approach used in [9], in which specialized hydrodynamic programs are applied for accurate modeling of the near explosion zone and the initial phase of shock wave propagation in the soil (for example, CTH, AUTODYN that were developed in the USA). However, the middle and far explosion zones are not studied, but protective structures are located at these distances, so these studies cannot be used to solve the problem.

The main tool for analyzing the soil-structure interaction is numerical modeling using the following methods.

The finite element method and the finite difference method are the most common ones for modeling the dynamic response of a structure. They are used to model the nonlinear behavior of the soil at high strain rates. Damage Models and plasticity models (for example, the Cap-Player model or the Johnson-Holmquist model) are used to simulate the compaction, shear, and possible liquefaction of the soil under wave action [10]. However, issues related to the interaction of the soil mass with the obstacle under explosive loads remain unresolved.

The smoothed particle hydrodynamics method and the discrete element method are used to model the failure and fragmentation of materials, especially in rock masses or in the analysis of the failure of a protective shell. The assessment of stability and damage is based on the application of different criteria. The displacement/velocity-based criteria most often use the peak particle velocity, the permissible levels of which for underground structures are usually higher than for above-ground structures, but more stringent criteria are applied to equipment inside the structure [11]. The shell deformation criterion is critical for tunnels and determines the risk of cracks or deflections leading to loss of load-bearing capacity. The damage-based criteria use the concept of accumulated material damage (e.g., concrete damage according to the Holmquist-Stewart model) to predict the degree of shell failure. The shortcomings of the work include the lack of a description of the process in the coupled formulation of the soil-obstacle system and simplified rheological models of the considered environments.

Experimental studies are necessary to obtain reliable dynamic parameters of materials and validate numerical models.

Work [12] reports the results of full-scale field tests using real explosive charges: measured pressure and velocity profiles in the soil (using accelerometers, peak velocity meters) and the stress-strain state of the shell (using strain gauges).

Paper [13] reports the results of scaled-up experiments using reduced-scale models of structures, following the laws of similarity. These tests are more cost-effective and allow for more control over variables (e.g., soil type, embedment depth).

Laboratory tests of dynamic properties of soil and concrete are described in [14]. To determine the behavior of materials at high strain rates (from 10^{-1} to 103 s^{-1}), a Split Hopkinson Pressure Bar was used, which allowed the authors to obtain stress-strain curves for materials under a dynamic mode. This is critically important for numerical modeling.

Works [12–14] are useful for comparing the results of numerical calculations with experimental data, but these data are limited to specific soil conditions, structure models, and types of explosive charges.

Current research is actively developing innovative approaches to increasing the stability of protective structures under dynamic loads. Protective layers of foam concrete or geosynthetic materials are introduced between the soil and an obstacle. These layers are designed to dissipate the energy of the blast wave and reduce the load transmitted to the main structure [15]. Composite materials (fiber concrete and polymer composites) are used to increase the plasticity and resistance of the obstacle to cracking and fragmentation. Structures made of monolithic soils (jet grouting technology) that form soil-cement screens are being investigated. The shape of underground structures is being optimized [16].

Thus, the following conclusions can be drawn from our analysis of literary sources. Analytical methods do not make it possible to obtain regularities in the evolution of wave processes for different soil conditions and explosion parameters [8]. In numerical modeling, the near zone of the explosion and the initial phase of the shock wave propagation in the soil are studied in detail [9], while the middle and far zones are ignored. Issues related to the interaction of the soil mass with an obstacle under explosive loads remain unresolved [10]. There is no description of the process in the coupled formulation of the "explosion products-soil-obstacle" system and simplified rheological models of the considered media are applied [11]. At the same time, simplified rheological models of the considered media are used in the above works. Experimental studies [12–14] are useful for comparing the results of numerical calculations with field data, which are limited by specific soil conditions, structure models, and types of explosive charges. The development of practical innovative approaches to increasing the stability of protective structures under dynamic loads [15, 16] requires further advancement of a reliable assessment of the stability of protective soil-cement structures in the soil massif under the action of critical explosive influences.

The above review of the literature [1–16] allows us to state that it is advisable to conduct a study aimed at detailed determination of the stress-strain state of the soil massif and soil-cement protective structure under the action of critical explosive loads. In this case, it is necessary to investigate wave processes in the coupled system "explosion products-soil massif-obstacle" using modern environment

models. This will make it possible to more reliably assess the stability of underground structures protected by a soil-cement screen under different explosion parameters, depths of installation, as well as compile practical recommendations regarding its component composition.

3. The aim and objectives of the study

The purpose of our work is to determine stability of a protective soil-cement structure in the soil under the action of critical explosive effects; this will make it possible to control the parameters of jet cementing at different depths of laying and explosion scales.

To achieve the goal, the following tasks were set:

– to construct a model of the stress-strain state of the system "detonation products - soil - soil-cement barrier";

– to investigate the patterns of interaction between explosive waves and the soil mass and soil-cement protective structure depending on the mass of the warhead, the depth of laying, and the distance from the epicenter of the explosion;

– to establish the dependence of stability of the soil-cement barrier on the cement content and to build a nomogram for practical calculation of stability of protective structures at different depths of laying under the explosive action of warheads of different masses.

4. The study materials and methods

The object of our study is the dynamic interaction between the soil and an obstacle under the explosive load of warheads of different masses.

The main hypothesis assumes that wave processes occur in the connected system "detonation products-soil massif-protective structure". This is due to the fact that only in such a setting can a complete picture of the propagation, departure, and interaction of waves be obtained, which ultimately will provide more reliable information for predicting stability of the protective structure. In addition, it is assumed that the soil and soil-cement obstacle are studied within the framework of a modern model of a solid, porous, multicomponent, viscoplastic medium with a variable coefficient of bulk viscosity, which most fully reflects the mechanisms of dynamic deformation.

To determine the stress-strain state of the soil massif and protective structure, the equation of motion of a continuous medium was used. With the addition of rheological equations of state of detonation products, soil and soil-cement barrier and the corresponding initial and boundary conditions, a closed system of partial differential equations was built.

To solve the task, the finite difference method was used in a moving Lagrangian coordinate system with a moving grid that automatically expands at the end of each computational cycle. A finite-difference scheme of the "cross" type with artificial viscosity was used [17]. This approach allowed us to conduct end-to-end calculations both on smooth flows and on discontinuities (shock waves reflected from the surfaces of the wave medium interface).

To construct the dependences, the information and analytical software MS Excel (developed in the USA) was used.

Calculations were performed for soil with the following physical and mechanical characteristics:

$\rho_{20} = 1{,}000$, $\rho_{30} = 2{,}650$ kg/m^3;

$c_{20} = 1{,}500$, $c_{30} = 4500$ m/s;

$\gamma_2 = 7$, $\gamma_3 = 4$; $\rho_0 c_S^2 = 3{\cdot}10^6$,

$\rho_0 c_D^2 = 1.2 \cdot 10^7$, $\rho_0 c_{SR}^2 = 3{\cdot}10^6$ Pa;

$m = 3$; $k = -1.5 \cdot 10^7$ Pa;

$\gamma_S = 6$; $\gamma_D = 7$; $\gamma_{SR} = 7$;

$\eta_D = 200$ Pa·s; $\alpha_1 = 0.1$;

$\alpha_2 = 0.3$; $\alpha_3 = 0.6$; $\rho_0 =$,1620 kg/m^3.

The physical and mechanical properties of a soil-cement barrier are as follows: $\alpha_1 = 0.04–0.3$; $\alpha_2 = 0$; $\alpha_3 = 0.7–0.96$: $\rho_0 = 2000$ kg/m^3, $\tau = 2$ MPa.

Cast TNT with the following characteristics was used as the explosive: $P_n = 9.6 \cdot 10^9$ Pa, $\rho_n = 1{,}600$ kg/m^3, $Q = 4.87 \cdot 10^6$ J/kg, $N = 3.12$; $\gamma = 0.25$; $D = 6{,}440$ m/s [16].

To solve the task set, the finite-difference method was chosen in a moving Lagrangian coordinate system with a moving grid that automatically expands at the end of each computational cycle using a finite-difference scheme of the "cross" type [15].

5. Results of investigating stability of the protective structure in the soil massif under the action of explosive influences

5. 1. Model of the stress-strain state of the system "detonation products-soil-soil-cement barrier"

The explosion of a TNT warhead of cylindrical shape with a length l and a radius r_0 in the soil massif on a free surface was considered. It is assumed that upon impact with the soil, the warhead detonates instantly, and the detonation products throughout the volume have the same density ρ_n, equal to the initial density of the explosive (EX), and the pressure P_n. In the Cartesian coordinate system rOz, the cylindrical volume is formed as a result of the rotation of a rectangle with sides l and r_0 around the z axis (Fig. 1).

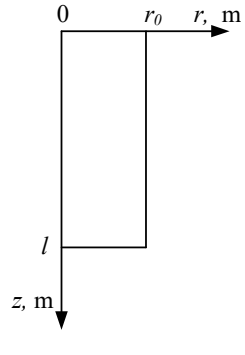

Fig. 1. Experimental model

The equations of motion within the framework of continuum mechanics for the system "detonation products-soil-obstacle" for cylindrical symmetry take the following form [15]:

$$\frac{\partial \sigma_{rr}}{\partial z} + \frac{\partial \tau_{rz}}{\partial r} + \frac{\tau_{rz}}{r} = \rho \frac{du}{dt}, \; u = \frac{dz}{dt}, \tag{1}$$

$$\frac{\partial \tau_{rz}}{\partial z}+\frac{\partial \sigma_{zz}}{\partial r}+\frac{\sigma_{zz}-\sigma_{\theta\theta}}{r}=\rho\frac{dw}{dt},\ w=\frac{dr}{dt}, \tag{2}$$

$$\frac{1}{V}\frac{dV}{dt}=\frac{\partial u}{\partial z}+\frac{\partial w}{\partial r}+\frac{w}{r}, \tag{3}$$

$$\sigma_{zz}=S_{zz}-P,\ \sigma_{rr}=S_{rr}-P,\ \sigma_{\theta\theta}=S_{\theta\theta}-P, \tag{4}$$

$$P=\frac{1}{3}\left(\sigma_{rr}+\sigma_{\theta\theta}+\sigma_{zz}\right),\ V=\frac{\rho_0}{\rho},$$

where t is time; ρ is density; u, w are velocity components; P is mean hydrostatic pressure; V is relative specific volume; σ_{rr}, $\sigma_{\theta\theta}$, σ_{zz} are normal stresses; τ_{zr} is tangential stress; S_{zz}, S_{rr}, $S_{\theta\theta}$ are components of the stress tensor deviator.

The soil and the soil-cement structure (obstacle) are modeled by a solid, porous, multicomponent, viscoplastic medium with a variable coefficient of bulk viscosity [17]. The equation of soil compression and unloading takes the following form

$$\dot{\varepsilon}=\phi\left(P,\varepsilon\right)\dot{P}-\frac{\alpha_1\lambda\left(P,\varepsilon\right)}{\eta\left(P,\varepsilon\right)}\psi\left(P,\varepsilon\right). \tag{5}$$

The functions included in equation (5) for the load are:

$$\phi\left(p,\varepsilon\right)=\alpha_1\left(\frac{df_D}{d\varepsilon_1}\right)^{-1}-\sum_{i=2}^{3}\alpha_1 B_1\left[A_1\left(P-P_0\right)+1\right]^{-k_i-1},$$

$$\lambda\left(p,\varepsilon\right)=1-\left(\frac{df_D}{d\varepsilon_1}\right)^{-1}\frac{df_S}{d\varepsilon_1},$$

$$\psi\left(p,\varepsilon\right)=P-P_0-f_S\left(\varepsilon_1\right), \tag{6}$$

$$f_S\left(\varepsilon_1\right)=A_S^{-1}\left[\left(\varepsilon_1+1\right)^{-\gamma_S}-1\right],$$

$$f_D\left(\varepsilon_1\right)=f_S\left(\varepsilon_1\right)+k\varepsilon_1,\ \kappa<0,$$

$$\varepsilon_1=\frac{1}{\alpha_1}\left(\varepsilon-\sum\nolimits_{i=2}^{3}\alpha_i\varepsilon_i\right)=$$

$$=\frac{1}{\alpha_1}\left\{\varepsilon+1-\sum\nolimits_{i=2}^{3}\alpha_i\left[A_i\left(P-P_0\right)+1\right]^{-k_i}\right\}-1,$$

$$A_i=\frac{\gamma_i}{\rho_{i0}c_{i0}^2},\ B_i=\frac{1}{\rho_{i0}c_{i0}^2},\ k_i=\frac{1}{\gamma_i},\ i=2,3;\ A_S=\frac{\gamma_S}{\rho_0 c_S^2},$$

where ρ_{i0}, c_{i0} – densities and sound speeds of liquid and solid components at atmospheric pressure P_0; γ_i – exponents in Theta-type equations for these components; ρ_0 – initial density of the medium at P_0; c_S, γ_S – sound speed and exponent in the volume compression equation under static loading.

When the medium is unloaded, the values of the functions take the following form:

$$\phi\left(P,\varepsilon\right)=\alpha_1\left[\frac{df_D}{d\varepsilon_1}-\frac{df_S}{d\varepsilon_1}+\frac{df_{SR}}{d\varepsilon_1}\right]^{-1}-$$

$$-\sum_{i=2}^{3}\alpha_i B_i\left[A_i\left(P-P_0\right)+1\right]^{-k_i-1},$$

$$\lambda_1\left(P,\varepsilon\right)=\left(\frac{df_D}{d\varepsilon_1}-\frac{df_S}{d\varepsilon_1}\right)\left(\frac{df_D}{d\varepsilon_1}-\frac{df_S}{d\varepsilon_1}+\frac{df_{SR}}{d\varepsilon_1}\right)^{-1},$$

$$\psi\left(p,\varepsilon\right)=P-P_0-f_{SR}\left(\varepsilon_1\right),$$

$$f_S\left(\varepsilon_1\right)=A_S^{-1}\left[\left(\varepsilon_1+1\right)^{-\gamma_S}-1\right],$$

$$f_D\left(\varepsilon_1\right)=f_S\left(\varepsilon_1\right)+k\varepsilon_1,\ \kappa<0, \tag{7}$$

$$f_{SR}\left(\varepsilon_1\right)=$$

$$=A_{SR}^{-1}\left\{\left\{\varepsilon_1+1+\left[A_{SR}\left(P_m-P_0\right)+1\right]^{-1/\gamma_{SR}}-\right\}^{-\gamma_{SR}}-1\right\},$$

$$\left\{-\left[A_S\left(P_m-P_0\right)+1\right]^{\frac{-1}{\gamma_S}}\right\}$$

$$P_m-P_0=A_S^{-1}\left[\left(\varepsilon_{1m}+1\right)^{-\gamma_S}-1\right],\ k_i=\frac{1}{\gamma_i},\ \ i=2,3;$$

$$A_S=\frac{\gamma_S}{\rho_0 c_S^2},\ \ A_{SR}=\frac{\gamma_{SR}}{\rho_0 c_{SR}^2}.$$

The variable coefficient of bulk viscosity has the form:
– under load [18]

$$\eta\left(P,\varepsilon\right)=\eta_D\left\{\frac{P-P_0-\frac{\rho_0 c_S^2}{\gamma_S}\left[\gamma_S\varepsilon_1-1+\left(\varepsilon_1+1\right)^{-\gamma_S}\right]}{\varepsilon_1\left(k-\rho_0 c_S^2\right)}\right\}^{-m}; \tag{8}$$

– when unloading [19]

$$\eta\left(\varepsilon\right)=\eta_D\times$$

$$\times\left\{\frac{P-P_0-A_{SR}^{-1}\left\{\left\{\varepsilon_1+1+\left[A_{SR}/A_S\left(\varepsilon_{1m}+1\right)^{-\gamma_S}+1\right]^{-\gamma_{SR}}-\left[\left(\varepsilon_{1m}+1\right)^{-\gamma_S}+1\right]^{-\gamma_S}\right\}^{-\gamma_S}-1\right\}}{\varepsilon_1\left(k-A_{SR}^{-1}\right)}\right\}^{-m}.$$

The components of the soil stress deviator were determined by the following relations:

$$S_{rr}=-\left(y_o+\frac{k_\tau P}{1+\frac{k_\tau P}{\tau-y_o}}\right),\ S_{\theta\theta}=-\frac{1}{2}S_{rr},$$

$$S_{zz}=\frac{2\left(1+k_\tau\right)}{1+2k_\tau}P,\ \tau_{rz}=k_\tau\left|\sigma_{rr}-\sigma_{zz}\right|, \tag{9}$$

where y_o is the soil cohesion, k_τ is the coefficient of internal friction, τ is the ultimate shear strength.

The expansion of detonation products occurred according to a binomial isentrope

$$P=A\rho^N+B\rho^{\gamma+1}, \tag{10}$$

where A, B, N, and Y are constants that define this type of EX.

The initial conditions of the problem are as follows:

$$u=0,\ w=0,\ P=P_n,\ \rho=\rho_n \text{ at } z\le l,\ r\le r_0, \tag{11}$$

$$u=0,\ w=0,\ P=P_0,\ \rho=\rho_0 \text{ at } z>l,\ r>r_0. \tag{12}$$

The boundary conditions are the continuity of the normal components of the velocity and stress vectors at the contact boundaries "PD-soil" and "soil-obstacle", as well as the condition $\sigma_{zz} = \tau_{zr} = 0$ met on the free surface.

5. 2. Regularities in the interaction between blast waves and the soil massif with soil-cement protective structure

As a result of numerical modeling, the following results were obtained. Fig. 2, *a, b* shows the isobars of the average hydrostatic pressure (GPa) in the plane at different times.

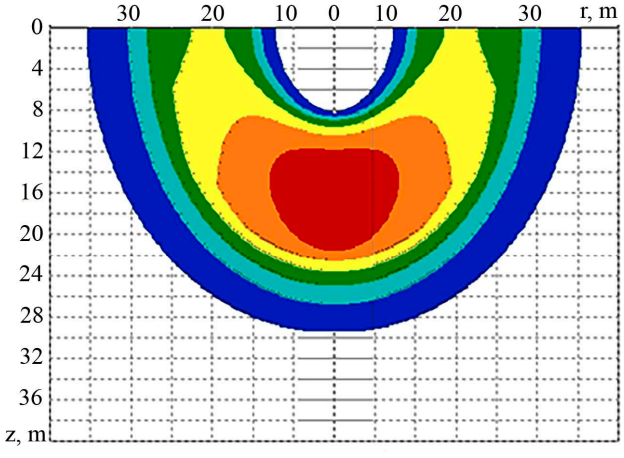

a

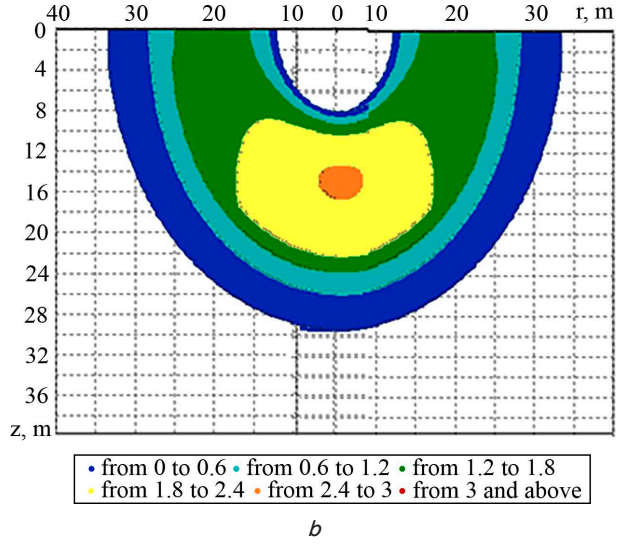

b

Fig. 2. Stress isobars σ_{rr} (MPa) at different times during the explosion of a cylindrical warhead at different times: *a* – $t = 0.05$ s; *b* – $t = 0.1$ s

From Fig. 2 it is seen that the isobar field is a complex pattern, caused by the interaction between waves with different boundaries and corner points, as well as with each other. At the initial time, the highest pressure is reached in the gas cavity and in the soil near it. There is a gradual degeneration of the wave front from cylindrical to spherical. The wave pattern becomes more complicated when propagating along the soil surface. In the flow region behind the front of the main shock wave, several secondary waves can be distinguished in the explosion products. One of them is reflected from the axis of symmetry, and the other propagates towards it, causing pressure pulsations, which, in turn, will lead to an increase in soil deformation.

Fig. 3 shows isoseisms of velocity u (m/s) at different times, from which it is possible to observe the propagation of the wave deep into the soil massif with a simultaneous decrease in its velocity.

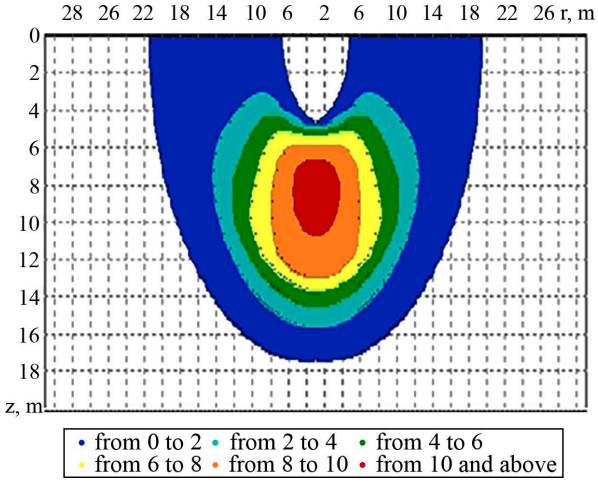

a

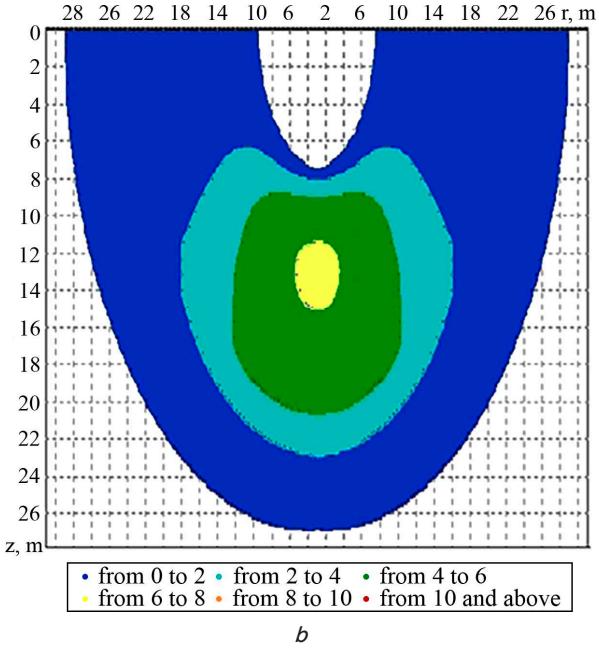

b

Fig. 3. Isoseisms of velocity u (m/s) at different times during the explosion of a cylindrical charge at different times: *a* – $t = 0.05$ s; *b* – $t = 0.1$ s

The dependence of peak stress on depth for different charge masses is shown in Fig. 4.

Plots of the exponential decay of peak stress with increasing depth Z were constructed (Fig. 4). It can be seen that at a small depth (0–2 m) the stress drops very sharply. This is a zone of plastic deformations and possible crushing (the zone where the soil-cement barrier was located). Further (from 5 m) the rate of decay slows down, and the stress turns into a typical seismic wave, transmitted over longer distances, but with a much smaller amplitude. This confirms why the soil-cement barrier at a depth of 2 m is very vulnerable – it is located precisely in the zone of the largest and fastest stress drop. And if we con-

sider that the compressive strength of the soil-cement barrier is 2–5 MPa, then from the analysis of the graphical dependence we can conclude that it will be destroyed at a depth of 2 m.

With an increase in the mass of the charge to 150 kg, the critical depth required to prevent complete crushing of the soil-cement barrier increases to ≈ 5.3 meters. If the barrier is at a shallower depth, it will be destroyed even without horizontal displacement of the charge.

Fig. 5 shows pressure fields at different times when the wave falls on the soil-cement barrier.

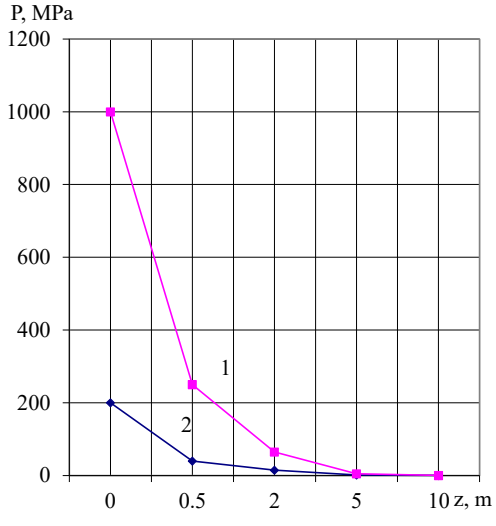

Fig. 4. Dependence of peak stress on depth for different charge masses: 1 — 150 kg; 2 — 50 kg

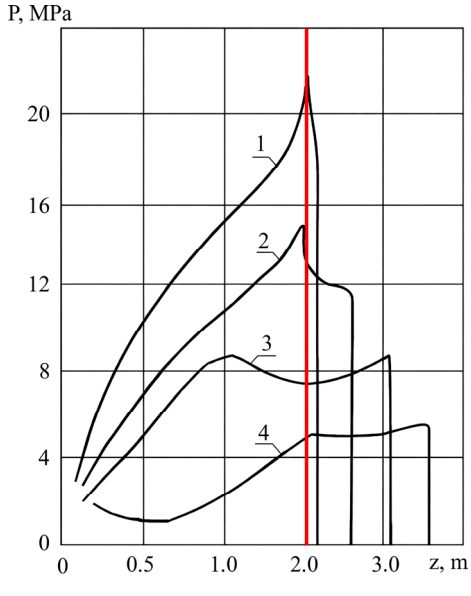

Fig. 5. Pressure fields during the explosion of a 50 kg TNT charge at different times when the soil-cement barrier is located at a depth of 2 m: 1 — $t = 5.2 \cdot 10^{-3}$ s; 2 — $t = 5. \cdot 10^{-3}$ s; 3 — $t = 6.7 \cdot 10^{-3}$ s; 4 — $t = 7.1 \cdot 10^{-3}$ s

It is known that the nature of the reflection of the incident wave from the interface of the layers will be different depending on their physical and mechanical properties. In this case, the second medium is denser; therefore, it has greater acoustic rigidity. Hence, the reflected wave will be impact. Fig. 4 shows that when the incident wave approaches the "soil-obstacle" interface, the pressure in it increases sharply. With increasing time, the reflection coefficient increases. The maximum pressure is at the front of the passing shock wave, and the minimum at the "detonation products-soil" rupture contact. As the wave propagates along the obstacle, the peak value decreases, but its oscillations can be observed, which causes oscillations of the soil-cement obstacle (Fig. 6).

From Fig. 6 it is established that although the pressure on the obstacle decreases with time, the deflection at the frontal point increases. This is explained by the fact that the behavior of the obstacle is elastic-plastic since the pressure in the incident wave causes stresses in the frontal point of the obstacle exceeding its elastic limit and causes plastic deformations. These deformations can cause the destruction of the obstacle with such a close location of the charge.

From Fig. 7 it is established how the distance from the epicenter of the explosion of a soil-cement obstacle affects the peak pressure values.

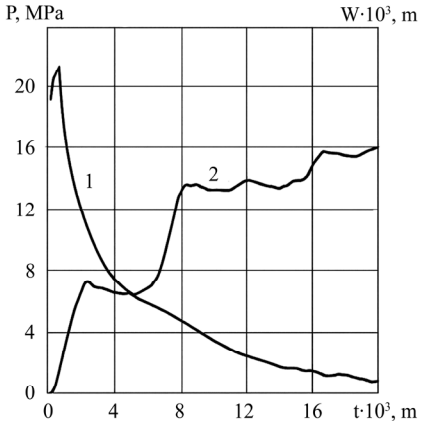

Fig. 6. Time dependences on the median surface at the frontal point of an obstacle during the explosion of a 50 kg TNT warhead: 1 — pressure; 2 — deflection

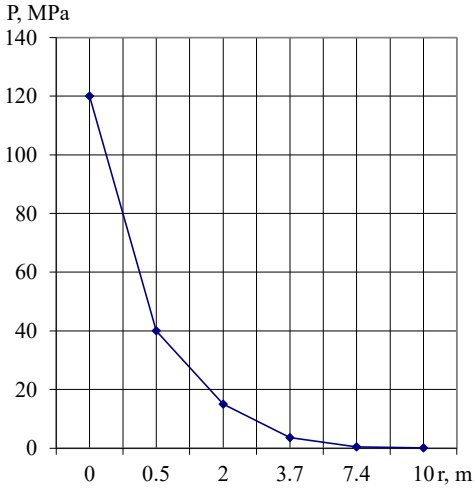

Fig. 7. Dependence of peak stress $\sigma_{max}(r)$ on horizontal distances during the explosion of a 50 kg TNT charge

From the plot in Fig. 7, it is established that the peak stress decreases rapidly with distance from the explosion center. For $R < 3.7$ m, the obstacle is in a zone of very high stresses ($\sigma_{max} > 2$ MPa), which leads to complete crushing and loss of shape. For $R \approx 7.4$ m, the stress drops to approximately 0.3–0.5 MPa. This is the threshold value for preserving the function of the soil-cement obstacle since it is close to its

tensile/shear strength limit. At $R > 10$ m, the stress decreases sharply, and the impact turns into a normal seismic oscillation, which is unlikely to cause significant structural damage.

This plot (Fig. 7) demonstrated that horizontal distance is a key factor in protecting underground fragile structures from surface explosions.

Therefore, it was investigated what the safe distance to the explosion epicenter was for an obstacle with a 2 m laying height for charges of different masses (Fig. 8).

As can be seen from the calculation (Fig. 8), with a decrease in the mass of the charge from 500 kg to 50 kg, the zone of safe horizontal distance decreases significantly, but even 50 kg of TNT is a very powerful destructive mechanism at distances less than 13.5 m.

Therefore, the question arose about the safe depths of laying soil-cement protective screens when detonating charges on the surface of the soil massif. In this case, various soils with densities from $\rho_0 = 1990$ kg/m^3 to $\rho_0 = 2485$ kg/m^{3}N will be considered, which covers the main types of soil conditions from sandy loam to clay. In work [17], it was established that during the explosion of an EX charge with an increase in soil porosity (decrease in density) there is a decrease in peak pressure, but at the same time the deformation increases. Fig. 9 shows the minimum safe depths for laying a soil-cement barrier depending on the mass of a charge for different types of soils.

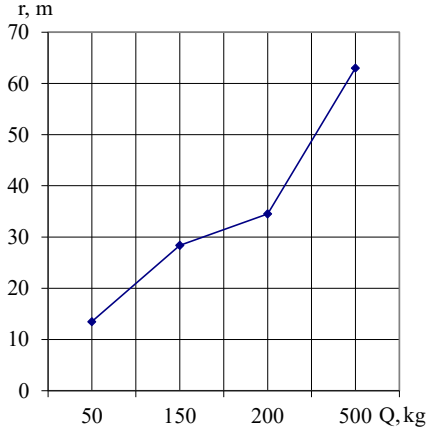

Fig. 8. Minimum safe horizontal distances to the epicenter of the explosion for a soil-cement barrier at a depth of 2 m in the soil massif depending on the mass of the charge

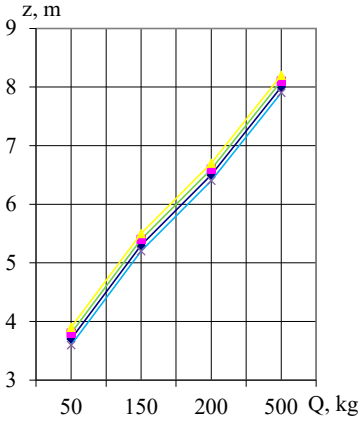

Fig. 9. Dependences of the minimum safe depth of laying a soil-cement barrier depending on the mass of a charge: $1 - \rho_0 = 1990$ kg/m^3, $2 - \rho_0 = 2155$ kg/m^3, $3 - \rho_0 = 2320$ kg/m^{3}N, $4 - \rho_0 = 2485$ kg/m^{3}N

As can be seen from our calculations (Fig. 9), with a decrease in the charge mass from 500 kg to 50 kg, the zone of intensive destruction decreases significantly. However, even 50 kg of TNT is powerful enough to cause complete crushing of the soil-cement obstacle if it is located at a distance of less than 3.7 meters from the epicenter of the explosion.

Increasing the depth of the obstacle to 5 m for a 50 kg charge brought the obstacle out of the zone of complete crushing even when the explosion occurred directly above it. To maintain its functionality, it is enough to carry the charge to a horizontal distance of more than 5.4 m.

With an increase in the charge mass to 150 kg, the critical depth required to prevent complete crushing of the soil-cement obstacle increases to ≈5.3 meters. If the obstacle is located at a shallower depth, it will be destroyed even without horizontal displacement of the charge.

Increasing soil porosity requires the obstacle to be placed at a greater depth. With a 20% decrease in soil density, the critical depth increased by 15%.

5. 3. Dependence of soil-cement barrier stability on cement content, laying depth, and warhead mass

A nonlinear relationship between soil-cement strength and the amount of added binder has been established, which is based on the classical theory of hardening of binders, adapted to the specifics of the soil environment. The main theoretical basis for the calculation is Abrams's Law, which postulates a direct dependence of concrete strength on cement content [20].

The more cement, the higher the strength, but this dependence is not infinite and has its economic and technical limits. Sandy soils interact best with cement; even with a 5–7% content, sufficiently high strength can be obtained. Clay soils require more cement (10–14%) due to the high specific surface area of particles and the need to neutralize clay minerals. With a cement content of more than 12–15%, the material becomes too stiff. This led to the appearance of "reflected" cracks in the upper layers of soil cement due to high hydration shrinkage. Increasing the cement content from 5% to 10% provided a 2–3-fold increase in strength, while a further increase to 15% would give an increase of only 30–50% and could, with further increase, form a system of cracks. Thus, the recommended cement content in a protective soil cement structure was determined to be appropriate to be taken within 10–15%.

From the above patterns, calculations were carried out for cement contents of 8, 15, and 30% according to the methodology given in [20].

Fig. 10 shows the dependence of compressive strength τ of a soil cement barrier on cement content (%).

Based on the results of our calculations, a nomogram was constructed to determine the mechanical properties of a soil-cement barrier located at a certain depth during a surface explosion of a warhead of a certain mass depending on the cement content (Fig. 11). In this case, curves 1 and 2 are shown in Fig. 3, and curve 3 is shown in Fig. 10. A common scale was used for the peak pressure P and compressive strength of the soil-cement barrier. The use of the nomogram makes it possible to control the stability of the protective structure by adjusting the parameters of the jet cementation of soils.

From this nomogram, we can calculate the composition of the soil-cement (cement content) when laying the obstacle at different depths. For example, if it is necessary to place the

obstacle at a depth of 2 m when a 50 kg warhead explodes, then following line 1, we find the peak pressure P and the corresponding compressive strength of the soil-cement obstacle and then determine the cement content in %.

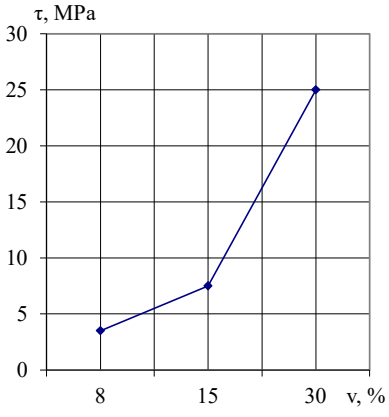

Fig. 10. Dependence of compressive strength τ of a soil-cement barrier on cement content (%)

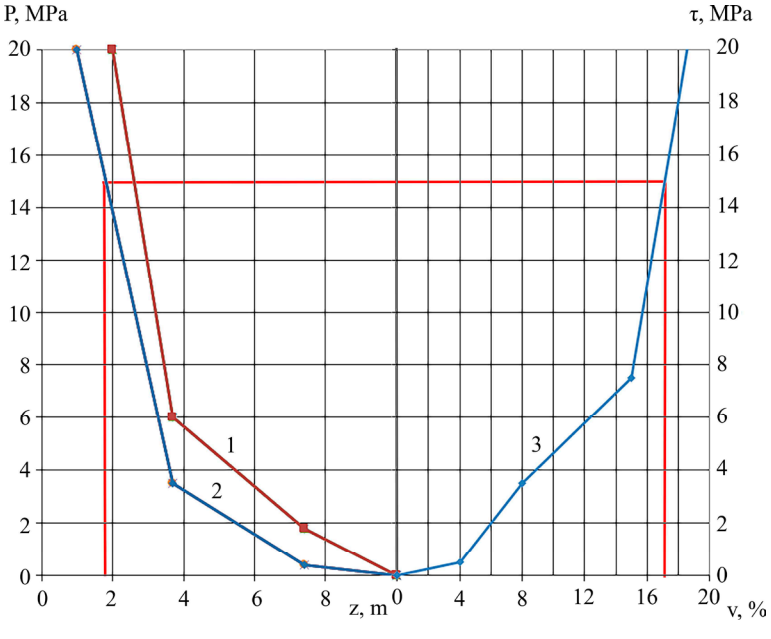

Fig. 11. Nomogram for calculating the cement content (%) in a soil-cement obstacle when it is located at different depths for different warhead masses: 1 — 150 kg; 2 — 50 kg; 3 — dependence of the compressive strength of an obstacle on cement content

6. Discussion of results based on investigating the stability of a protective underground structure under the action of critical explosive loads

Our results, in particular the stress isobars (Fig. 2) and velocity isoseisms (Fig. 3) are related to a well-founded mathematical model of the stress-strain state of the system "detonation products – soil – soil-cement barrier" (1) to (12), which correctly reflects the processes of dynamic interaction under the specified conditions.

Analysis of the research results allows us to trace the exponential decrease of the peak stress with increasing depth (Fig. 7). At a small depth (up to 2 m), the stress decreases very sharply. This is a zone of plastic deformations and possible crushing (the zone where the soil-cement barrier was placed). Further (from 5 m), the rate of decrease slows down, and the stress turns into a typical seismic wave, which is transmitted over longer distances, but with a much smaller amplitude. This explains why the soil-cement barrier at a depth of 2 m is very vulnerable – it is located precisely in the zone of the largest and fastest stress drop. And if we take into account that the compressive strength of soil-cement is 6–8 MPa, we can conclude that its destruction is highly probable at a depth of up to 2 m (even with a minimum warhead mass of 50 kg). With an increase in the mass of the charge to 150 kg, the critical depth required to prevent the destruction of the soil-cement barrier increases to 5.3 m (if the barrier is located at a shallower depth, it will be destroyed) (Fig. 9). Classical methods that use empirical and semi-empirical dependences [8, 13] do not make it possible to obtain regularities of wave processes for different soil conditions and explosion parameters.

It was found that the peak stress decreases rapidly with distance from the epicenter of the explosion (Fig. 8). For $R < 3.7$ m, the screen (obstacle) is in the zone of high tensile stresses ($\sigma_{max} > 2$ MPa), which leads to crushing, loss of shape, and stability of the structure. For $R \approx 7.4$ m, the tensile stress decreases to approximately 0.3–0.5 MPa. These values should be considered as a threshold value for preserving the holding (protective) function of the soil-cement obstacle, since it approaches the tensile or shear strength limit of the soil-cement. At $R > 10$ m, the stress decreases sharply, and the impact turns into a normal seismic oscillation, which is unlikely to cause noticeable structural damage. Unlike well-known works [10, 12, 14], which investigate the protective properties of the reinforced concrete frame of underground structures under the action of explosive influences, our task considered the impact of a protective screen. At the same time, unlike [10, 12], which investigate protective concrete screens laid on the surface, our results substantiate a more promising direction of the formation of soil-cement protective structures, the appropriate depth of placement of which is determined by our studies.

Thus, the prospects of engineering protection of underground facilities by forming a continuous soil-cement screen in the path of the blast wave, formed by jet cementing of soils, have been proven.

Among the limitations of this study, it should be noted that the modeling of explosive effects in the form of detonation of a charge from the free surface is important. Actual air strikes from unmanned aerial vehicles or cruise missiles add energy and angle of incidence to the critical effects, as well as the effect of a certain immersion of the warhead in the soil before the explosion. These effects can enhance the destructive effect of the warhead by 10–15% [5] (in this case, we are not talking about special types of warheads for the destruction of underground facilities).

The disadvantages of the study include the simplification associated with the fact that the protective structure is laid in the form of a soil-cement barrier, but most real protective structures have more complex geometric and physical-mechanical properties.

Further advancement of the research is associated with the addition of a directly underground structure with differ-

ent geometric, structural, and mechanical parameters to the considered system "detonation products - soil - soil-cement barrier". This is necessary for a comprehensive assessment of protective capabilities of the soil-cement screen and the reinforced concrete frame of the structure.

7. Conclusions

1. A model of the stress-strain state of the system "detonation products-soil-soil-cement barrier" has been built. Special feature of the model is the study on the dynamics of fields in the coupled system of the considered media and the application of a modern soil model with variable viscosity. For the analysis, the finite-difference method was used in a moving Lagrangian coordinate system with a moving grid that automatically expands at the end of each computational cycle using a finite-difference scheme of the "cross" type and a method for numerically solving the problem of the explosion of a cylindrical projectile in a soil mass near the free surface, taking into account the interaction with a soil-cement barrier (screen). This allowed us to study the stress-strain state and the patterns of change in wave processes in the soil mass and barrier depending on the time of impact, the mass of the charge, and the depth of the screen.

2. By modeling, the isobar field of the average hydrostatic pressure during the explosion of a cylindrical warhead at different times and velocity isoseisms were obtained. They reveal the regularities of wave propagation deep into the soil massif and changes in its velocity and pressure (exponential decrease of peak stress with increasing depth). The wave pattern during propagation along the soil surface becomes more complicated. In the flow region behind the front of the main shock wave, several secondary waves can be distinguished in the explosion products. One of them is reflected from the axis of symmetry, and the other propagates towards it, causing pressure pulsations, which, in turn, leads to an increase in soil deformation. The dependence between the pressure and the deflection of the protective soil-cement structure (obstacle) has been determined, which makes it possible to predict the stability of protective screen at different depths of installation. The optimal depth of laying the soil-cement screen with a charge weight of 50 kg should exceed 2 m, with a weight of 150 kg – 5.3 m.

3. Based on the results of our calculations, a nomogram was constructed to determine the mechanical properties of the soil-cement barrier under the action of critical loads depending on cement content. The use of the nomogram makes it possible to control stability of the protective structure by adjusting parameters for the jet cementation of soils.

Conflicts of interest

The authors declare that they have no conflicts of interest in relation to the current study, including financial, personal, authorship, or any other, that could affect the study and the results reported in this paper.

Funding

The study was carried out within the framework of research work "Risk modeling and protection against critical impacts of urban underground infrastructure and civil defense structures" (State registration number – 0124U000912, source of funding – Ministry of Education and Science of Ukraine).

Data availability

All data are available in the main text of the manuscript.

Use of artificial intelligence

The authors confirm that they did not use artificial intelligence technologies when creating the current work.

Authors' contributions

Natalia Remez: conceptualization, Methodology, Software, Validation, Formal Analysis, Writing – original draft, Writing – review & editing, Supervision, Project administration; **Hennadii Haiko:** Conceptualization, Validation, Formal analysis, writing – original draft, Writing – review & editing, Supervision, Project administration; **Vadym Bronytskyi:** Conceptualization, Methodology, Software; Writing – review & editing, Visualization; **Tetiana Hrebeniuk:** Investigation, Writing – review & editing; **Svitlana Haiko:** Investigation, Writing – review & editing.

References

1. Remez, N., Bronytskyi, V., Hrebeniuk, T. (2024). Risk assessment for the development of the exemplified territories. POWER ENGINEERING: Economics, Technique, Ecology, 1. https://doi.org/10.20535/1813-5420.1.2024.300835
2. Remez, N., Dychko, A., Bronytskyi, V., Hrebeniuk, T., Bambirra Pereira, R., Ekel, P. (2021). Simulation of the influence of dynamic loading on the stress-strain state of the natural and geoengineering environment. E3S Web of Conferences, 280, 01008. https://doi.org/10.1051/e3sconf/202128001008
3. Remez, N. S., Dychko, A. O., Hrebeniuk, T. V., Kraichuk, S. O., Pereira, R. B. (2022). Interaction behaviors of longitudinal and transverse seismic waves with underground objects. Book of Abstracts of the 3rd International Conference on Sustainable Futures: Environmental, Technological, Social and Economic Matters, 25. Available at: https://www.igns.gov.ua/wp-content/uploads/2022/05/book-of-abstracts_icsf-2022.pdf
4. Haiko, H., Savchenko, I., Shelestov, A. (2025). Ensuring resilience and safety of the transportation system of Kyiv in planning the network of road tunnels. Case Studies on Transport Policy, 19, 101355. https://doi.org/10.1016/j.cstp.2024.101355
5. Haiko, H., Hollander, J. B., Savchenko, I. (2025). Priority ranking of alternative Odesa metro plan variants: using modified morphological analysis method. International Journal of Urban Sciences, 29 (4), 910–938. https://doi.org/10.1080/12265934.2025.2452509

6. Lin, Q., Feng, C., Gan, Y., Yuan, J., Jiao, W., Yang, Y. (2024). Study of Difference in Dynamic Response of Underground Structure at Different Blast Angles. Advances in Frontier Research on Engineering Structures II, 393–401. https://doi.org/10.1007/978-981-97-6238-5_32
7. Krauthammer, T. (2008). Modern Protective Structures (Civil and Environmental Engineering). CRC Press. Available at: https://openlibrary.org/books/OL8125346M/Modern_Protective_Structures_%28Civil_and_Environmental_Engineering%29
8. UFC 3-340-02. Structures to Resist the Effects of Accidental Explosions (2008). Washington. Available at: https://www.wbdg.org/FFC/DOD/UFC/ARCHIVES/ufc_3_340_02.pdf
9. Belytschko, T., Liu, W. K., Moran, B., Elkhodary, K. I. (2014). Nonlinear finite elements for continua and structures. John Wiley & Sons. Available at: https://download.e-bookshelf.de/download/0004/0349/97/L-G-0004034997-0002588474.pdf
10. Johnson, G. R., Holmquist, T. J. (1993). A computational constitutive model for concrete subjected to large strains, high strain rates, and high pressures. In: 14th International Symposium on Ballistics. Available at: https://ftp.lstc.com/anonymous/outgoing/jday/concrete/scanned_mat111.pdf
11. Dowding, C. H. (2000). Construction Vibrations. Upper Saddle River, NJ: Prentice Hall. Available at: https://openlibrary.org/books/OL8526402M/
12. Mandal, J., Agarwal, A. K., Goel, M. D. (2020). Numerical Modeling of Shallow Buried Tunnel Subject to Surface Blast Loading. Journal of Performance of Constructed Facilities, 34 (6). https://doi.org/10.1061/(asce)cf.1943-5509.0001518
13. Zhou, Q., He, H., Liu, S., Chen, X., Tang, Z., Liu, Y. et al. (2021). Blast resistance evaluation of urban utility tunnel reinforced with BFRP bars. Defence Technology, 17 (2), 512–530. https://doi.org/10.1016/j.dt.2020.03.015
14. Kolsky, H. (1949). An Investigation of the Mechanical Properties of Materials at very High Rates of Loading. Proceedings of the Physical Society. Section B, 62 (11), 676–700. https://doi.org/10.1088/0370-1301/62/11/302
15. Zhao, H., Yu, H., Yuan, Y., Zhu, H. (2015). Blast mitigation effect of the foamed cement-base sacrificial cladding for tunnel structures. Construction and Building Materials, 94, 710–718. https://doi.org/10.1016/j.conbuildmat.2015.07.076
16. Remez, N. S., Dychko, A. O., Sini, L., Minaieva, Yu. Yu. (2025). Recovery of bombturations and unstable soils by drilling mixing technology. Scientific Notes of Taurida National V.I. Vernadsky University. Series: Technical Sciences, 2 (1), 284–290. https://doi.org/10.32782/2663-5941/2025.1.2/41
17. Remez, N. S. (2019). Vzaiemodiya vybukhovykh khvyl z gruntamy i elementamy tekhnourbosystem. Kyiv: Tsentr uchbovoi literatury, 334.\
18. Remez, N., Haiko, H., Dychko, A., Boiko, V., Haiko, S., Antoniuk, O. (2024). Development of a mathematical model of dynamic soil deformation taking into account the variable coefficient of volumetric viscosity. E3S Web of Conferences, 567, 01010. https://doi.org/10.1051/e3sconf/202456701010
19. Remez, N., Haiko, H., Hrebeniuk, T., Woźniak, G. (2025). Assessment of the risks of dispersion of harmful gases during the detonation of non-Tentyl emulsion explosives. IOP Conference Series: Earth and Environmental Science, 1457 (1), 012020. https://doi.org/10.1088/1755-1315/1457/1/012020
20. Horpibulsuk, S., Rachan, R., Chinkulkijniwat, A., Raksachon, Y., Suddeepong, A. (2010). Analysis of strength development in cement-stabilized silty clay from microstructural considerations. Construction and Building Materials, 24 (10), 2011–2021. https://doi.org/10.1016/j.conbuildmat.2010.03.011